A numerical study of momentum and forced convection heat transfer in a rectangular channel with wall-mounted waved baffles

Etude numérique de l'écoulement et de transfert de chaleur par convection forcée dans un canal rectangulaire muni de chicanes ondulées

Younes Menni*, Ahmed Azzi & Chafika Zidani

Research Unit of Materials and Renewable Energies, Department of Physics, Faculty of Sciences, Abou Bekr Belkaid University, BP 119-Tlemcen, 13000, Algeria.

Soumis le 03/06/2015 *Révisé le 27/03/2016* *Accepté le 14/06/2016*

ملخص

أجريت في هذاالبحث دراسة رقمية لتحليل الجريان المضطرب وانتقال الحرارة داخل مجرى هوائي مستطيل الشكل يحتوي على أجنحة عرضية ولوحات حاجزة متموجة متصلة كليا بالجدران الداخلية للقناة. الهواء يعتبر مائعا مضطربا نيوتونيا، غير قابل للانضغاط خواصه ثابتة. كما تم دراسة خصائص الحمل الحراري المضطرب تحت تأثير عامل تغير قيمة عدد رينولدز من 5000 إلى 20000. المعادلات التفاضلية المرتكزة على نموذجk-ωSST لوصف الجريان الاضطرابي والواصفة للتدفق حلت بالتكامل و ذلك باستخدام خوارزمية SIMPLE والتي تعتمد على طريقة الحجوم المتناهية لحل المعادلات الجبرية التي تعتبر متداخلة فيما بينها (درجة الحرارة والسرعة وأيضا التغير المحوري للضغط والسرعة).

بالأخص، حقول السرعة ودرجة الحرارة، منحنيات السرعة المحورية، أعداد نيوسالت وك ذا الضياع في الطاقة بالاحتكاك تم تمثيلها تحت عامل تبوث درجة حرارة الجدران السفلية والعلوية للمجرى الهوائي.تم فحص دقة النتائج الرقمية من خلال المقارنة مع النتائج الرقمية وك ذا التطبيقية المنشورة.النتائج المحصل عليها بينت أساسا أن تدفق الهواء يمتاز بتشوه متموج حاد في المسار وبمناطق إعادة تدوير ضخمة وبصفة عامة، عدد نيوسالت ومعامل الاحتكاك تزداد بزيادة عدد رينولدز.

كلمات افتتاحية: الحجوم المتناهية - الجريان الاضطرابي - الحمل الحراري - أجنحة عرضية متموجة.

Résumé

Des caractéristiques d'écoulement turbulent et de transfert de chaleur par convection forcée ont été examinées pour un fluide (air) à propriétés constantes qui s'écoule à travers une conduite rectangulaire avec des chicanes ondulées et une température constante le long des parois. Le nombre de Reynolds est pris variable, 5,000-20,000. Les équations gouvernantes, basées sur le modèle *k-ω* SST, sont résolues par la méthode des volumes finis à l'aide de l'algorithme SIMPLE. En particulier, les champs de vitesse et de température, les profils de vitesse axiale, les nombres de Nusselt local et moyen, ainsi que les frottements ont été traités le long du canal à condition de température de parois constante. Les résultats obtenus ont été comparés à ceux obtenus par l'expérience dans la littérature. Ces résultats montrent essentiellement que l'écoulement est caractérisé par des fortes déformations et de grandes régions de recirculation. En général, le nombre de Nusselt et la friction augmentent avec le nombre de Reynolds.

Mots clés: *Volumes finis - Ecoulement turbulent - Convection forcée - Chicanes ondulées.*

Abstract

A numerical study has been carried out to examine the momentum and turbulent forced-convection characteristics for airflow through a constant temperature-surfaced rectangular duct with top and lower wall-mounted waved baffles.Air is the working fluid with the flow rate in terms of Reynolds numbers ranging from 5,000 to 20,000.The governing equations were integrated by the finite volume method, in two-dimensions, employing the SIMPLE-algorithm with the SST*k-ω* model to describe the turbulence. In particular, velocity and temperature fields, axial velocity profiles, local and average Nusselt numbers, and skin frictions were obtained at constant wall temperature condition along the top and bottom walls. The validation of the present code is done by comparing the present results with the published ones. The results reveal essentially, that the flow is characterized by strong deformations and large recirculation regions. In general, Nusselt number and friction loss increase with the Reynolds number.

Key words: *Finite volume method - Turbulent flow - Forced convection - Waved baffles.*

* *Corresponding author: menniyounes@gmail.com*

1. INTRODUCTION

Improvement of heat transfer in thermal devices such as heat exchangers and electronic equipments became an important factor in industry. For this purpose, various techniques have been proposed as the use of treated surfaces, rough surfaces, extended surfaces, surface vibration, fluid vibration, jet impingement, staggered or in-line baffles, flat or shaped baffles, vertical or inclined baffles, solid or porous baffles, fins, blocks, corrugated channel, coiled tubes, twisted tape inserts, discontinuous crossed ribs and grooves. Most of these enhancement techniques are based on the baffle arrangement. Use of heat transfer enhancement techniques lead to increase in heat transfer coefficient but at the cost of increase in pressure drop.

Fins and baffles submitted to laminar and turbulent flows have being analyzed in the recent years by several authors, using numerical and/or experimental techniques. The first work on the numerical investigation of flow and heat transfer characteristics in a duct with the concept of periodically fully developed flow was conducted by Patankar et al. [1]. The numerical investigation of fluid flow and heat transfer characteristics in a smooth channel with staggered baffles, based on the periodically fully developed flow conditions of Patankar et al. [1], was reported by Webb and Ramadhyani [2]. Kellar and Patankar [3] computed the heat transfer in channels with staggered baffles and found that the heat transfer increases with the rise in baffle height and with the decrease in baffle spacing. Their results showed the same behavior as Webb and Ramadhyani [2] results. An academic study on this topic was firstly reported by Berner et al. [4] who reported the effect of baffle presence in a shell and tube heat exchanger model using an approximate two-dimensional model. The turbulent flow and heat transfer between a periodical series of conducting parallel plates with surface-mounted heat sources were reported by Kim and Anand [5]. They found that the presence of the plates as baffles in electronic cooling channels would affect directly the friction factor and the Nusselt number and lead to an increase in heat transfer rate. Conjugate heat transfer in a rectangular channel with lower and upper wall-mounted obstacles was investigated by

Mohammadi Pirouz et al. [6] using the Lattice Boltzmann Method (LBM). In that study, the effects of Reynolds numbers, thermal diffusivity ratios, and the distance between obstacles, which are prescribed as multiples of obstacle width, were investigated.Dutta and Dutta [7] carried out both experimental and numerical studies. Their results show effects of inclined baffles on friction loss and heat transfer of turbulent flow in a rectangular channel with constant heat flux on the upper wall. The baffle size, orientation and perforation on the average and local Nusselt numbers were also reported. They found that the size, positioning and orientation of the baffle have significant influence on internal cooling heat transfer. In addition, an optimum perforation density for perforated baffles leads to strong jet impingement phenomenon and maximizes heat transfer. The numerical investigations of laminar forced convection in a three-dimensional channel with baffles for periodically fully developed flow and with a uniform heat flux in the top and bottom walls were presented by Lopez et al. [8]. Guo and Anand [9] studied the three-dimensional heat transfer in a channel with a single baffle in the entrance region. Numerical studies for both solid and porous baffles in a two dimensional channel for the turbulent flow (Yang and Hwang [10]) and for the laminar flow regimes (Da Silva Miranda et al. [11], and Santos and De Lemos [12]) were conducted, including the report on similar thermal performance. From the experiment for turbulent channel flow with porous baffles of Ko and Anand [13], the porous baffles are found to present a flow behavior as good as the one with solid baffles. Tsay et al. [14] investigated numerically by using baffles for enhancement of heat transfer in laminar channel flow over two heated blocks mounted on the lower plate. Sripattanapipat and Promvonge [15] studied numerically the laminar periodic flow and thermal behaviors in a two-dimensional channel fitted with staggered diamond-shaped baffles and found that the diamond baffle with half apex angle of 5-10° performs slightly better than the flat baffle.

Promvonge et al. [16] also examined numerically the laminar heat transfer in a square channel with 45° angled baffle placed on one wall. They reported that a single streamwise vortex flow occurs and induces impinging jets on the wall of the inter-baffle cavity and the baffle trailing edge (BTE) sidewall. Tang and Zhu [17] investigated experimental and numerical for flow of water

and heat transfer characteristics in a rectangular channel with discontinuous crossed ribs and grooves. They reported that the overall thermo-hydraulic performance for ribbed-grooved channel is increased by 10%-13.6% when compared to ribbed channel. The effects of wire coil, circular ring and twisted tape on heat transfer and pressure drop were reported by Eiamsa-ard [18,19]. The highest thermal enhancement factor was found at 1.42 for combined turbulator, circular ring and twisted tape.

Most of the previous investigations on turbulent flow have only considered the fluid flow and heat transfer characteristics for various baffle height and spacing ratios for porous, solid, transverse or inclined baffles in a channel. In consequence, the study on waved-shaped baffles in rectangular channel has rarely been reported. In the present work, the numerical computations for two-dimensional turbulent forced convection channel flows over a waved-shaped baffle pair mounted on two opposite walls are conducted with the main aim to examine the changes in the flow structure and heat transfer pattern. The employment of the waved-baffle placed periodically is expected to generate a pair of longitudinal vortex flows along the channel and give better mixing of fluid between the core and the wall region to result in higher heat transfer rate in the channel.

2. PHYSICAL MODELS

2.1. Computational domain

Steady two-dimensional turbulent forced convection flow in a constant temperature-surfaced rectangular channel with top and bottom wall-mounted waved-shaped baffles is numerically simulated.

Detail of the computational domain with the corrugated baffles and boundary conditions is shown in figure 1. This is the same test section described in Sripattanapipat and Promvonge [15] but the geometric parameters are modified. In that study, the laminar flow through a two-dimensionalhorizontal plane channel, where twodiamond-shaped baffles were placed in opposite walls, was numerically studied.
In this paper, the geometric properties of the given computational domain were based on the numerical and experimental data published by Demartini et al. [20]. In this work, the numerical simulations are conducted in a two-dimensional domain, which represents a rectangular channel of L=0.554m long and H=0.146m high, provided by two staggered corrugated baffles, through which a steady flow of turbulent air. The first is attached to the lower wall of the channel at distance of L_{in}=0.218m and the second inserted to the upper wall at L_{out}=0.174m from the outlet. The distance between the top of the corrugated baffle and the wall mother attachment is h=0.08m. The shape and dimensions of a corrugated baffle are also in figure 2. Also, a typical flat baffle pair with thickness of e=0.01m is introduced for validation (Fig. 3).

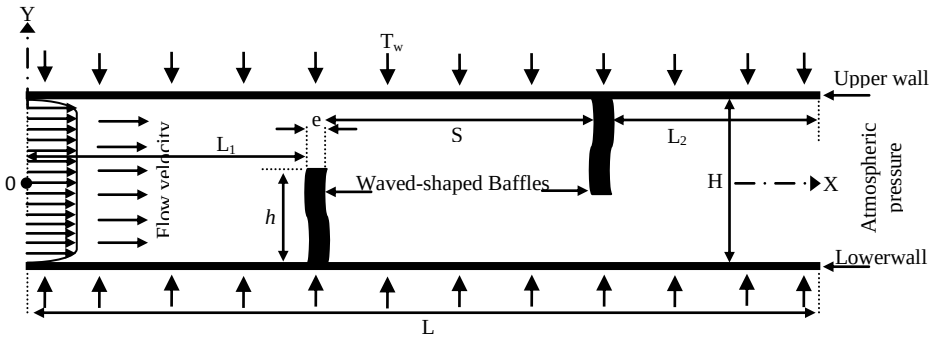

Figure 1. Detail of the test section with the corrugated baffles and boundary conditions.

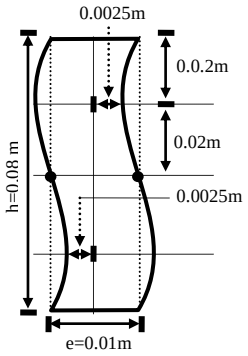

Figure 2: Geometry of corrugated baffle shape

2.2. Boundary conditions

The hydrodynamic boundary conditions are chosen according to the experimental work of Demartini et al. [20] while the thermal boundary conditions are set according to the numerical work of Nasiruddin and Kamran Siddiqui [21]. Air is the working fluidwith the flow rate in terms of Reynolds numbers ranging from 5,000 to 20,000.The boundary conditions were given as; (i) the air entered the channel at ambient temperature27°C (T_{in}=300K)with a uniform one-dimensional velocity ($u=U_{in}$, v=0); (ii) the pressure at the inlet of the computational domain was set equal to the zero (gauge); (iii) the turbulence intensity was kept at I=2% at the inlet; (iv) a constant temperature of 102°C (T_w=375K) was applied on the entire wall of the computational domain as the thermal boundary condition. (v) Impermeable boundary and no-slip wall conditions are imposed at the walls; and (vi) in the channel outlet (x=L) it is prescribed the atmospheric pressure ($P=P_{atm}$).

2.3. Numerical models

The numerical model for fluid flow and heat transfer in a rectangularchannel with wall-mounted corrugated baffles was developed under the following assumptions:

- Steady two-dimensional fluid flow and heat transfer.
- The flow is turbulent and incompressible.
- Constant fluid properties.
- Body forces and viscous dissipation are ignored.
- Negligible radiation heat transfer.

2.4. Grid system

Two-dimensional models of the corrugated baffled channel were created and calculation grids were generated by the GAMBIT 2.3 software program. Because the post-processing software FLUENT 6.3 [22] is more suitable for structured grids, the discretization of the entire computational domain was performed by adopting structured quadrilateral elements for the geometric model of the test computational domain.The grids adjacent to the baffled channel wall were refined. This refinement was necessary to resolve the strong velocity and temperature gradients in that region, as indicated bySripattanapipat and Promvonge [15], Demartini et al. [20], and Nasiruddin and Kamran Siddiqui [21]. For the regions more distant from the walls, the mesh is uniform, as presented by Demartini at al. [20].

The characteristics of four grids with 21100, 42300, 85000 and 171400cells are employed in the simulation to control the numerical model solution. The comparison shows that for the grid of size 85000 cells and above, the variation in average Nusselt numberand friction factor values for the given computational domain is less than 0.15%at the Reynolds number of 8.73×10^4. The above results show that the numerical solution does not depend on the meshsize and therefore, the final selected grid system is independentof the mesh size. An identical structured mesh systemis applied with the number of nodes equal to 200 and 425 (or 85000 cells) along the cross section and the length, respectively.Thegrid density was kept higher in the vicinity of the heatedwall and the corrugated baffles, as presented in more detail in Sripattanapipat and Promvonge [15], Demartini et al. [20], and Nasiruddin and Kamran Siddiqui [21]to capture the variations in the flowand temperature fields within the hydraulic and thermalboundary layers.

3. MATHEMATICAL FOUNDATION

Based on the above assumptions, the governing flow equations (i.e., continuity, momentum and energy equations) used to simulate the incompressible steady fluid flow and heat transfer in the given computational domain are given as

$$\frac{\partial u_j}{\partial x_j} = 0 \qquad (1)$$

$$\rho u_j \frac{\partial u_i}{\partial x_j} = -\frac{\partial P}{\partial x_i} + \frac{\partial}{\partial x_j}\left(\mu \frac{\partial u_i}{\partial x_j} - \rho \overline{u_i' u_j'}\right) \qquad (2)$$

$$\rho u_j \frac{\partial T}{\partial x_j} = \frac{\partial}{\partial x_j}\left((\Gamma + \Gamma_t)\frac{\partial T}{\partial x_j} \right) \quad (3)$$

Where ρ is the fluid density (constant); P is the pressure; μ is the dynamic viscosity; $u_i$and u_j are mean velocity components in $x_i$and $x_j$directions; u'_i and $u'_j$are fluctuation velocity components in $x_i$and x_j directions; Γ and Γ_t are molecular thermal diffusivity and turbulent thermal diffusivity, respectively and are given by

$$\Gamma = \frac{\mu}{\mathrm{Pr}} \quad \text{and} \quad \Gamma_t = \frac{\mu}{\mathrm{Pr}_t} \quad (4)$$

To ensure realistic and accurate turbulent modeling, the performance of four different turbulent models, namely Spalart-Allamaras model, k-ε model, k-ωmodel, and Reynolds Stress model were evaluated by solving Navier-Stokes equations. The comparison of the simulated results obtained by Nasiruddin and Kamran Siddiqui [21] from these turbulent models with the experimental data made the selection easy. The Shear-Stress Transport k-ω turbulent model which was proposed by Menter [24] was found to be the one that most accurately predicts the flow modification due to the baffle. The selected turbulent model is capable of calculating the rapidly evolving two-dimensional flow and also in predicting, interactions with the wall. Another advantage of the selected turbulent model is that the model equations behave appropriately in both the near-wall and far-field regions. The SST k-ωmodel is defined by two transport equations, one for the turbulent kinetic energy, k and the other for the specific dissipation rate ω, as given below [21,24]

$$\frac{\partial}{\partial x_i}(\rho k u_i) = \frac{\partial}{\partial x_j}\left(\Gamma_k \frac{\partial k}{\partial x_j} \right) + G_k - Y_k + S_k \quad (5)$$

$$\frac{\partial}{\partial x_i}(\rho \omega u_i) = \frac{\partial}{\partial x_j}\left(\Gamma_\omega \frac{\partial \omega}{\partial x_j} \right) + G_\omega - Y_\omega + D_\omega + S_\omega \quad (6)$$

where

$$G_k = -\rho \overline{u'_i u'_j} \frac{\partial u_j}{\partial x_i} \quad (7)$$

$$G_\omega = \alpha \frac{\omega}{k} G_k \quad (8)$$

and

$$\Gamma_k = \mu + \frac{\mu_t}{\sigma_k} \quad (9)$$

$$\Gamma_\omega = \mu + \frac{\mu_t}{\sigma_\omega} \quad (10)$$

In these equations, x_i and x_j are the spatial coordinates;G_k represents the generation of turbulence kinetic energy due to mean velocity gradients;G_ω represents the generation of ω;Γ_k and $\Gamma_\omega$represent the effective diffusivity of k and ω, respectively;Y_k and Y_ω represent the dissipation of k and ω due to turbulence;D_ω represents the cross-diffusion term;S_k and $S_\omega$are user-defined source terms.

FLUENT is the most powerful Computational Fluid Dynamics (CFD) software tool available, empowering you to go further and faster as you optimize your product performance. FLUENT includes well-validated physical modeling capabilities to deliver fast, accurate results across the widest range of CFD and multi-physics applications. In this simulation, The Commercial CFD software FLUENT 6.3, details of which can be found in Reference [22], was used to simulate the fluid flow and temperature fields. As a part of the same package, a preprocessor GAMBIT 2.3 was used to generate the required mesh for the solver. The governing equations were discretized using the Finite Volume Method (FVM), details of which can be found in Patankar[25]. The SIMPLE discretization algorithm [25] was used for the convective terms in the solution equations. The QUICK-scheme [25] was used to calculate the derivatives of the flow variables. To control the update of the computed variables at etch iteration, under-relaxation was varied between 0.3 and 1.0. The solutions were considered to be converged when the normalized residual values were less than 10^{-7} for all variables but less than 10^{-9} only for the energy equation.

Five parameters of interest in the present work are the Reynoldsnumber, skin friction coefficient, friction factor, and local and average Nusselt numbers. The Reynolds

number, Re, of the experiments [20] is Re=8.73×10^4, defined as

$$\mathrm{Re} = \frac{\rho \overline{U} D_h}{\mu} \quad (11)$$

where $\overline{U}$ is the mean axial velocity of the section velocity, 7.8 m/s, and D_h is the hydraulic diameter of the channel, equal to 0.167m. The skin friction coefficient,Cf is

$$Cf = \frac{2\tau_w}{\rho \overline{U}^2} \quad (12)$$

The friction factor, f, is computed by pressure drop, ΔPacross the length of the channel, L, as

$$f = \frac{(\Delta P / L) D_h}{\frac{1}{2}\rho \overline{U}^2} \quad (13)$$

The convective heat transfer is measured by local Nusselt number, Nu_x, which can be written as

$$Nu_x = \frac{h_x D_h}{\lambda_f} \quad (14)$$

The average Nusselt number, $\overline{Nu}$ can be obtained by

$$\overline{Nu} = \frac{1}{L}\int Nu_x \partial x \quad (15)$$

where τ_w the rate of shearing to the wall, and $h_x$the local convective heat transfer coefficient.

4. RESULTS AND DISCUSSION

4.1. Validation of numerical solution

The Finite VolumeMethod, by means of Commercial CFD software FLUENT 6.3 [22],is applied in this research work.To validate the numerical solution, the velocity profilesobtained from the present numerical simulations were comparedwith the mean velocity profiles from the experiments reported by Demartini et al.[20]fora rectangular-channel with upper and lower wall-mounted baffle plates.

Figure 3 shows the qualitative comparison between both velocity profiles. Both the experimental and numerical velocity profiles are computed along the height of the channel at axial location x=0.525m, near the channel outlet. For Re=8.73×10^4, the present numerical waved-baffled channel result is found to be ingoodagreement with numerical and experimental solution values obtained from Demartini et al. [20]. This provides a strong confidence in further simulation of the channel flow over the baffles.

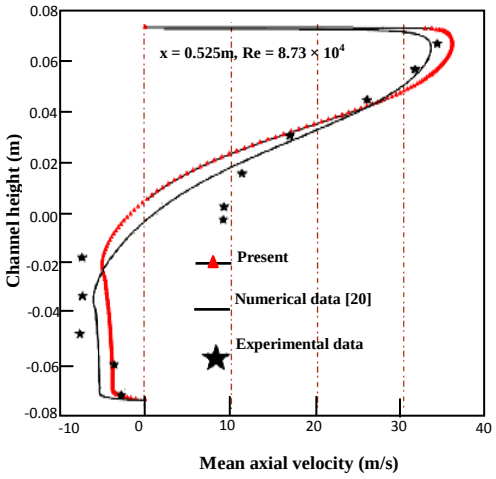

Figure 3. Comparison of axial velocity profiles obtained from the present work with those from experiments of Demartini et al. [20].

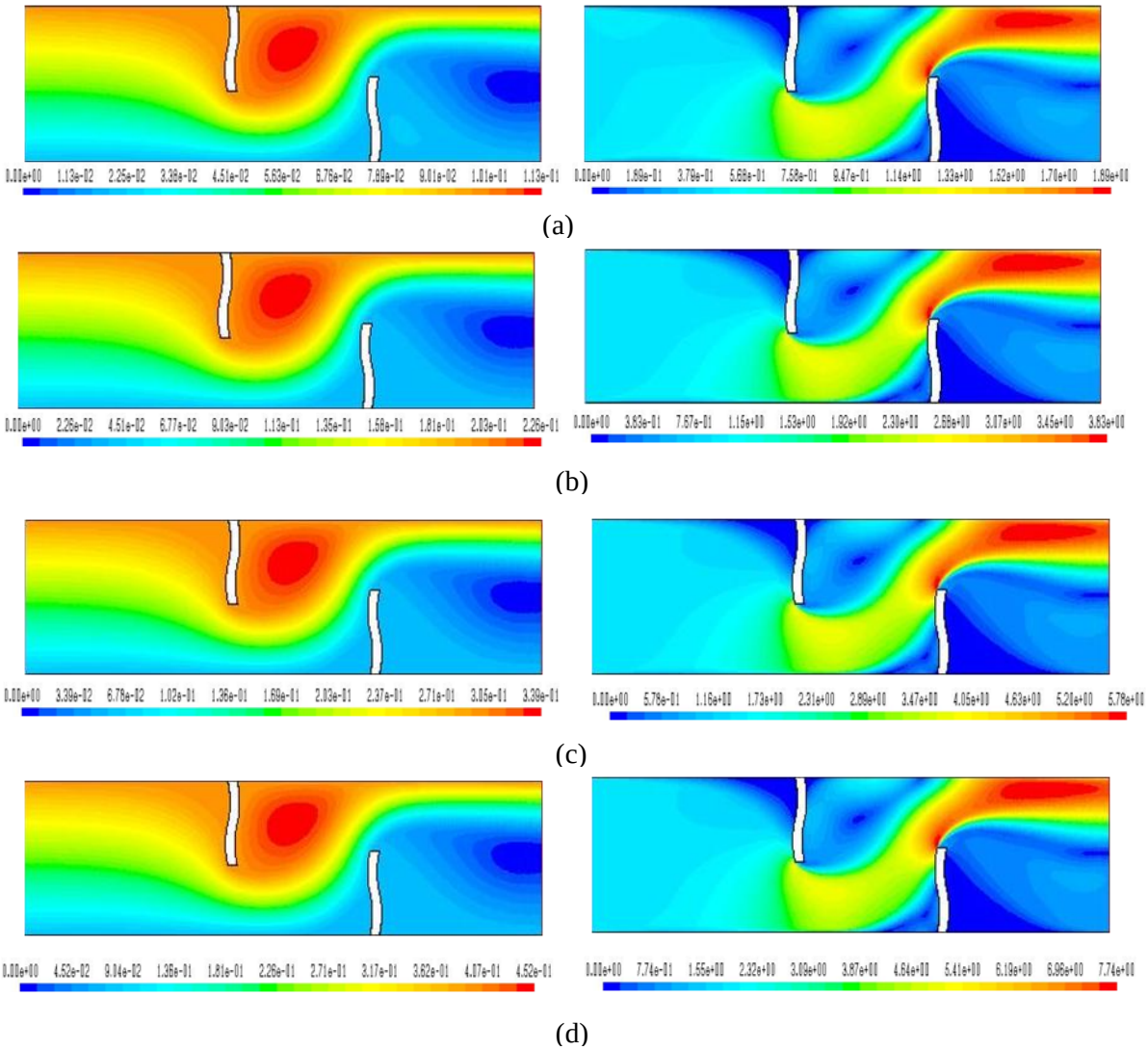

Figure 4. Variation of velocity magnitude fields and streamlines with Reynolds number: (a) Re=5.000, (b) Re=10.000, (c) Re=15.000 and (d) Re=20.000. Flow is from left to right.

4.2 Flow structure

Waved baffles play an important role in the dynamics of the flow through shell-and-tube heat exchangers. For the better comprehension of the phenomena produced by these devices, the search of detailed information about the flow characteristics is necessary. The flow structure in the presence of waved baffles could be easily discerned by considering the velocity magnitude and streamline plots as depicted in figure 4a, b, c and d for the cases of Re=5.000, 10.000, 15.000, and 20.000, respectively.

The comparison of streamlines at different Reynolds numbers shows that as the flow is accelerated and redirected near the corrugated baffles, a very small vortex is formed in the vicinity of the lower left corner. Downstream, as a result of sudden expansion in the cross-section, the flow separates, a larger clockwise vortex isformed behind the lower corrugated baffle and flow reattachment is then established. A similar phenomenon is observed near the corrugated baffle mounted on the upper wall with counterclockwise vortices at the upstream and downstream considered baffle, in accordance with the results showed by Mohammadi Pirouz et al. [6]. The velocity field magnitudes obtained for different values of Reynolds number are also shown in figure 4. In all cases, it is visible very low velocity values adjacent to the corrugated baffles. In the regions

downstream of both waved baffles, recirculation cells with very low velocity values are observed. In the regions between the tip of the considered baffles and the channel walls, the velocity is increased. Due to the changes in the flow direction produced by the corrugated baffles, thehighest velocity values appear near the lower channel wall with an acceleration process that starts just after the second waved baffle.These results showedthe same behavior as Demartini et al. [20] results except for flow areas around thebaffle corners.The variation of velocity profiles for all cases of Reynolds number appears clearly on the contours and their scales which present positive and negative values. For studying this dependence well, we plotted the axial velocity distribution for these transverse stations: x=0.159m, 0.189m, 0.255m, 0.285m, 0.315m, 0.345m and 0.525m. Figure 5 shows the axial distribution of velocity profiles at positions given by x=0.159m (see Fig.5a) and x=0.189m (see Fig.5b), respectively 0.059m before and 0.029m before the first corrugatedbaffle. In the figure, the influence of the deformation of the airflow field increases as the flow approaches the first waved baffle, increasing the velocity of the flow approaching the passage above the considered baffle. Figure 6 shows the evolution of axial velocity profiles for positions x=0.255m and x=0.285m, 0.027m and 0.057 m after the lower wall corrugatedbaffle. As seen from the figure, the flow is characterized by very high velocities at the upper part of the channel, approaching 315% of the inlet velocity, which is 0.45m/s (for example at Re=5.000), as shown in the position x=0.285m (see Fig.6b). In the upper part of the channel, negative velocities indicate the presence of recirculation behind the first baffle. The numerical results of axial velocity profiles for positions x=0.315m and x=0.345m, measured downstream of the entrance, are shown in figure 7a and b, respectively. These positions are located upstream of the second wavedbaffle, located at x=0.37m from the entrance. In the figures, it is visible that as the flow approaches the second corrugated baffle, its velocity is reduced in the upper part of the channel while in the lower part is increased. The presence of the negative values of the velocity again indicates the flow starts to accelerate toward the gap under the exit section of the channel.A presentation of numerical results of axial velocity profiles after the second corrugated baffle, near the channel outlet is given in figure 8. At a position x=0.525m, 29mm before channel outlet, the value of the velocity reaches 2.25m/s, 5 times higher than the entrance velocity (for example in the case of Re=5.000). These values are only possible due to the very strong flow recirculation on the back side of the second waved baffle, which leads air from outside of the channel into the test channel asindicated by Demartini et al. [20].The difference on the values of the velocity between our study and that of Demartini et al. [20]is due to the fact that we used in our investigation the corrugatedshape, whereas they used the flatshape of baffle plates. The variation plots of axial velocity distributions obtained for different values of Reare also shown in figures. 5-8. As expected, obviously it can be observed that values of velocity become higher with increasing values in Re. It is concluded that the presence of corrugated baffles leads to longer flow path and high strength of vortex due to changing in its orientation. The flow pattern of using different Re values looks similar except for flow areas around the waved baffle corners

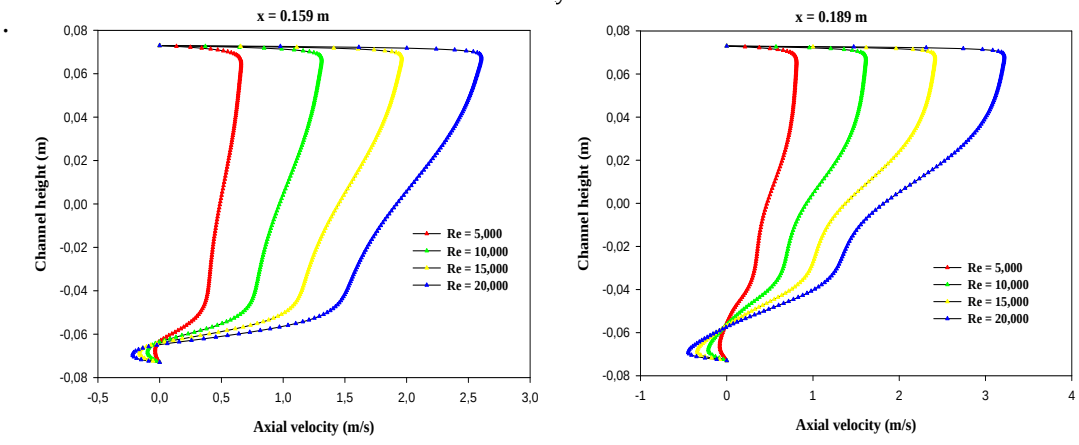

(a) (b)

Figure 5. Variation of axial velocity profiles with flow Reynolds number upstream of the first corrugated baffle for stations: (a) x=0.159m, and (b) x=0.189m.

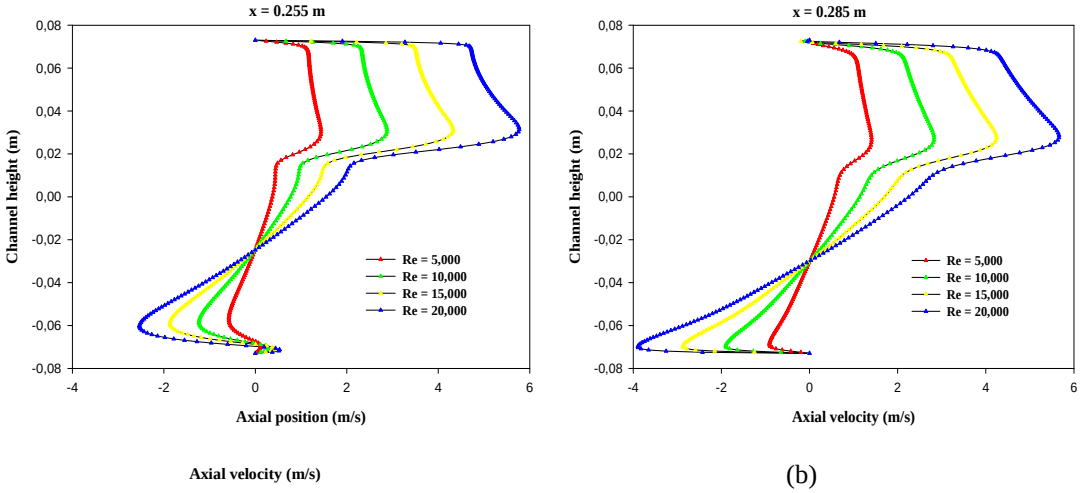

Axial velocity (m/s)

(b)

Figure 6. Variation of axial velocity profiles with flow Reynolds number between the first and the second corrugated baffles for locations: (a) x=0.255m, and (b) x=0.285m.

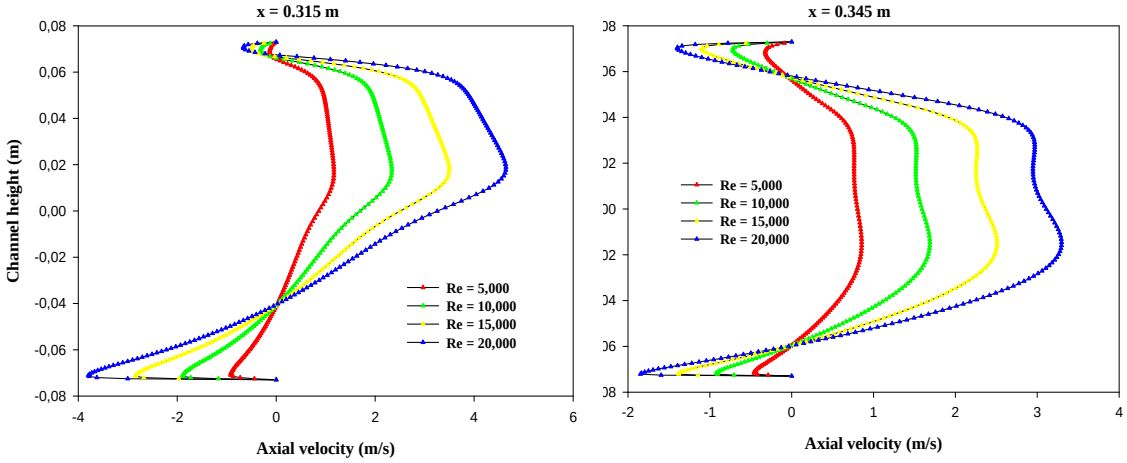

(a) (b)

Figure 7. Variation of axial velocity profiles with flow Reynolds number upstream of the second corrugated baffle for positions: (a) x=0.315m, and (b) x=0.345m.

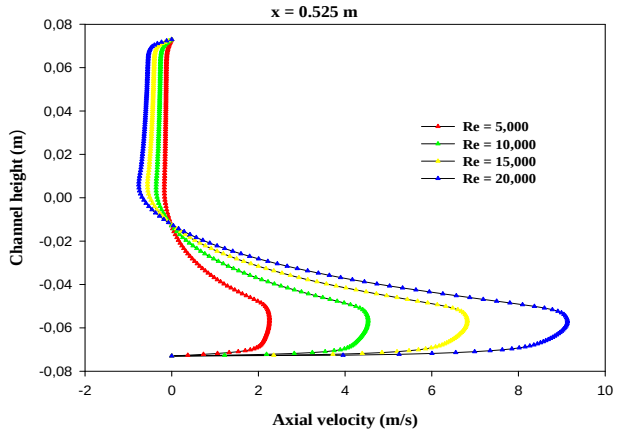

Figure 8. Variation of axial velocity profiles with flow Reynolds number after the second corrugated baffle, near the channel outlet.

4.3. Heat transfer

The presence of the corrugated baffles influences not only the velocity field but also the temperature distribution in the whole domain investigated.Numerical results of total temperature profiles versus the Reynolds number for locations x=0.189m, 0.255m, 0.345m, and 0.189m, measured downstream of the entrance, are shown in figure 9a-d, respectively. In the figure, it is interesting to note that the fluid temperature in the recirculation region is significantly high as compared to that in the same region of no corrugated baffle case, in accordance with the results reported byNasiruddin and Kamran Siddiqui [21].There is a major change in the temperature distribution along both channel walls, especially in the region opposite the

waved baffle tipasindicated bySripattanapipat and Promvonge [15]. This means that the vortex or recirculation zone provide a significant influence on the fluid temperature, because they can induce better fluid mixing between the wall and the core regions, leading to a high temperature gradient along the heating channel wall. The lower temperature values near the tip of the considered baffles are due to the high velocities in that region. The temperature distribution presented in figure 9 shows that the onset of the recirculation zones, near theheated wall has increased the fluid temperature. Therefore, it is reasonable to expect that a small corrugated baffle can effectively improve the heat transfer characteristics in a waved baffled exists between the corrugatedbaffles and performance improvements obtained that we describe in what follows. One notices a rapid decrease in the Nusselt number until reaching its minimum value the level of the base of these waved-baffles. This decrease is continuing with a low velocity until reaching values very close to zero, which explains practically, no heat exchange between the wall and fluid at this location. Then, the heat transfer rate increases significantly and rapidly along the corrugatedbaffle and reaches its maximum on its upper side because the velocity close to the bottom of the channel is strongly elevated (5 times the input velocity U_{in}) due to intense recirculation zone in the back face of the second considered baffle. It is concluded that the largest local convective heat transfer coefficient variations are found near the tip of the wavedbaffle, due to the strong velocity gradients in that region,in accordance with the results reported by Mohammadi Pirouz et al. [6], Sripattanapipat and Promvonge [15], and Nasiruddin and Kamran Siddiqui [21]. In the figure, the local Nusselt numbers are also related as a function of Re number. To increase the Reynolds number of the flow, the velocity of the air flow at the entrance of the channel was increased. This acceleration causes the increased the size of the recycling zones and consequently the local Nusselt number is found strongly affected by the change of the Reynolds number, (see Fig.10a and b). It was found that the highest rate of heat transfer is achieved by increasing the Reynolds number where the flow structure very disturbed which promotes mixing of the fluid. On each wall, when the Reynolds number increases, where we also find that the temperature gradientat the level of the heated walls increases with increasing flow rate. This channel. The plot also shows that the Reynolds number has a significant impact on the fluid temperature in the given channel. The flow was simulated for the Reynolds number of 5,000, 10,000, 15,000, and 20,000. The results indicate that for a given baffle setup, anincrease in the flow Reynolds number decreases the fluid temperature for all locations investigated.

The heat transfer rate, characterized by the local Nusselt number, is then determined and shown along the lower and upper inner surfaces of the channel in figure 10a and b, respectively. Nusselt numbers are calculatedfrom their definition as given in Eqs. (14) and (15).It is seen that all profiles have the same gait, which confirms once more the direct relationship that is because the introduction of the negative velocity of the turbulent flow, forced convection reduces the level of turbulence intensity within the boundary layer.

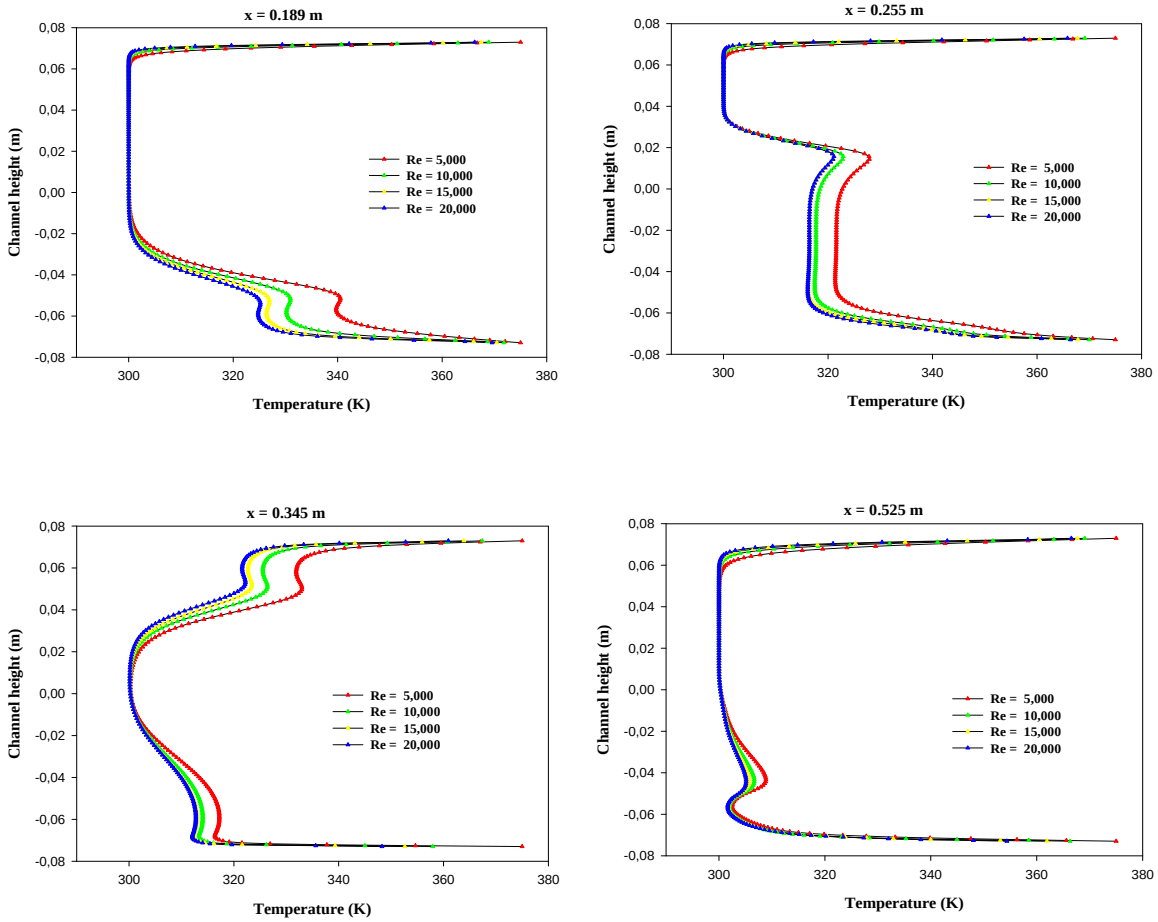

Figure 9: Variation plots of temperature profiles with flow Reynolds number for transverse sections:(a) upstream of the first wavedbaffle at x=0.189m, (b) between the first and the second corrugatedbaffles at x=0.255m, (c) upstream of the second considered baffle at x=0.345m, and (d) after the second baffle, near the channel outlet at x=0.525m.

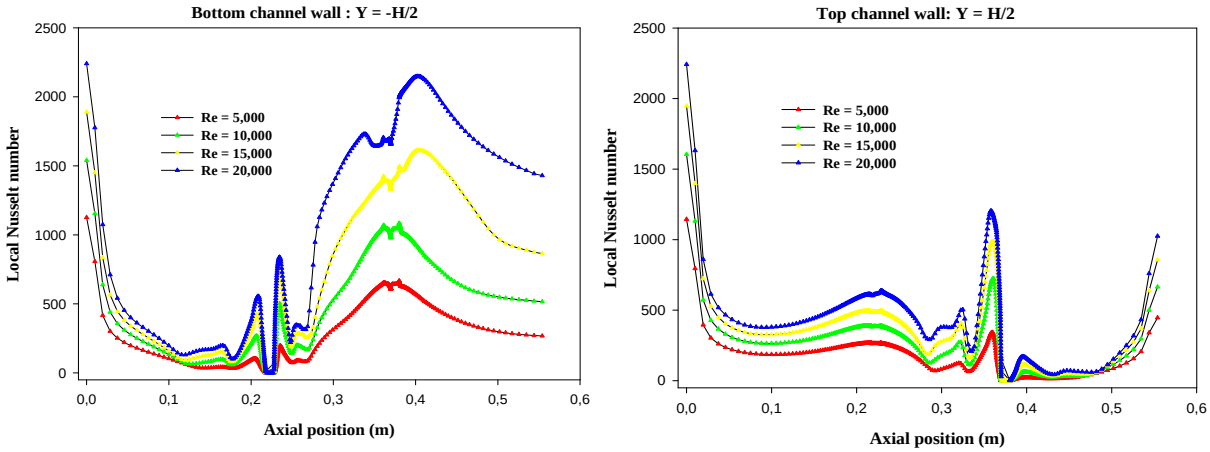

Figure 10. Variation plots of local Nusselt number profiles with flow Reynolds number at the surface of (a) lower and (b) upper walls of the channel.

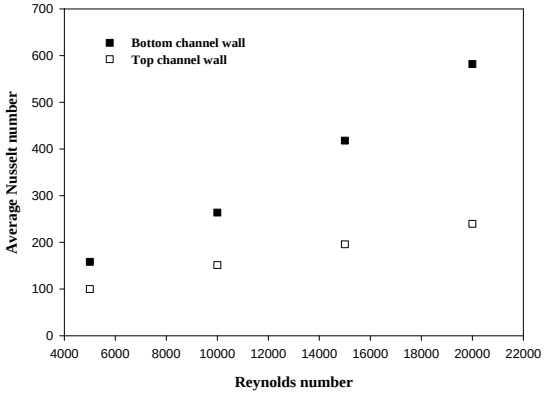

Figure 11: Variation of average Nusselt number with flow Reynolds number.

The influence of Reynolds number on the evolution of the average Nusselt number ispresented in figure 11 here it is shown an increase of the average heat transferby increasing Reynolds number due to the augmentation ofthe inertia forces further to the augmentation of the flow rate.As expected, the largest variations in the average Nusselt number are found at the bottom wall of the channel, due to thestrong velocity gradients in that region.

4.4. Friction loss

An important factor to be considered when using corrugated solid material for the purpose of heat transfer enhancement is the increased pressure drop. Local and average frictioncoefficients are calculatedfrom their definition as given in Eqs. (12) and (13), respectively.

The skin friction coefficient distribution along the channel at different Reynolds numbers is shown in figure 12a and b for both bottom and top channel walls, respectively. In the figure, it is evident that the presence of the corrugated baffles involves the increased value of surface friction on the channel wall. The skin friction coefficients are increased again at the locations corresponding to the zones of counter rotating flow as seen in the figure. It indicates that the highest skin friction coefficient can be observed at the area of high turbulent intensity especially at the top faces of the lower and upper wall baffles.Similarly to the results reported in previous investigations (Sripattanapipat and Promvonge [15]), two minimum friction coefficient values are generated by the separation of the flow through the baffle. One is around the baffle and the other is at reattachment point behind the baffle. Also, in the figure, the increase of skin friction coefficients is found to be larger than that of the heat transfer coefficients caused by the temperature field. This may imply that the flow field develops more rapidly than the temperature field. The trends of Cf are similar for all Re values, an increase in the flow Reynolds number causes a substantial increase in the Nusselt number but the pressure loss is very significant.

The variation of friction factor with Reynolds number for both lower and upper channel walls is plotted in figure 13. As expected, it is clear from this figure that the friction factor increases with the increase of the flow Reynolds number, and the highest pressure loss is obtained when the channel wall is y=-H/2 in which there is more flow resistance.

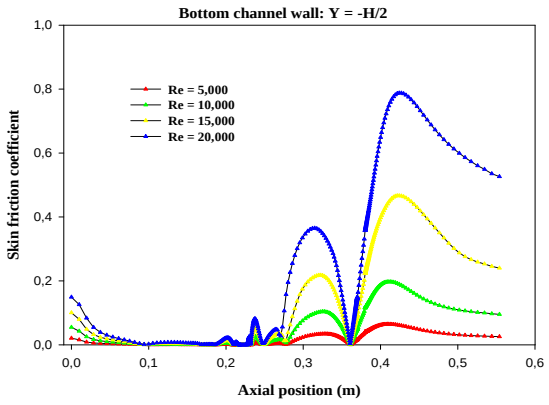

(a)

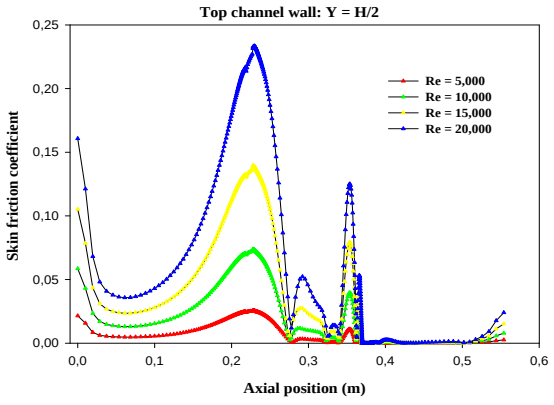

(b)

Figure 12. Variation plots of skin friction coefficient profiles with flow Reynolds number at the surface of (a) lower and (b) upper walls of the channel.

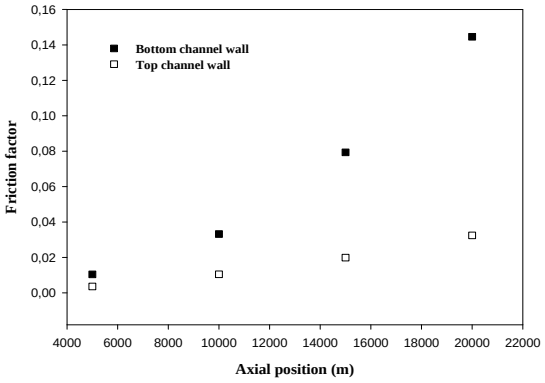

Figure 13. Friction factor versus Re

5. CONCLUSION

A detailed numerical study of the momentum and forced convection heat transfer characteristics of air through a two-dimensional horizontal rectangular cross section channel, where two waved baffles were placed in opposite walls, was carried out. All the governing equations were discretized by the QUICKnumerical scheme, decoupling with the SIMPLE-algorithm andsolved using a finite volume approach.For closure of theequations, the Shear Stress Transport k-ω modelwas used in the present study.Numerical calculations were performed with the Commercial CFD software FLUENT 6.3, in the range of Reynoldsnumber 5,000-20,000.The result was validatedwith available rectangular-baffle measured data and found to agree well with measurement.The following conclusions can be derived as:

- ✓ The air flows above, under and between the corrugated baffles by taking their exact shape with presence of recirculation zones downstream from each bafflewhose size increases by raisingthe Reynolds number value.
- ✓ The largest variations in the velocity field occur in the regions near to the corrugated baffles, as expected.
- ✓ Due to the changes in the flow direction produced by the corrugated baffles, the highest velocity values appear near the lower channel wall with an acceleration process that starts just after thesecond corrugated baffle.
- ✓ The higher temperature gradient can be observed where the flow impinges the channel wall while the lower one is found at the corrugated baffle corner area where the corner recirculationzone occurs, especially area behind the baffle.
- ✓ The airflow velocity value tends to increase with the rise ofReynolds number while the temperature showed an opposite trend, as expected.
- ✓ An increase in the flow rate in terms of Reynolds numberscauses a substantial increase in the heat transfer but the pressure loss is also very significant.
- ✓ The above results suggest that a significant heat transfer enhancement in a channel can be achieved by introducing a corrugatedbaffle pair into the flow.
- ✓ The conclusions of this paper are of great significancein the improvement of heat exchanger channel with waved baffles.
- ✓ These observations are confirmed by several authors, using numerical and/or experimental techniques as Mohammadi Pirouz et al. [6], Sripattanapipat and Promvonge [15],Demartini et al. [20], and Nasiruddin and Kamran Siddiqui [21].

REFERENCES

[1] Patankar S.V., Liu C.H., Sparrow E.M., 1977. Fully developed flow and heat transfer in ducts having streamwise-periodic variations of cross-sectional area, *ASME J. Heat Transfer*, Vol. 99, 180-186.

[2] Webb B.W., Ramadhyani S., 1985. Conjugate heat transfer in a channel with staggered ribs, *Int. J. Heat Mass Transfer*, Vol. 28, 1679-1687.

[3] Kelkar K.M.&Patankar S.V., 1987. Numerical prediction of flow and heat transfer in a parallel plate channel with staggered fins, *ASME J. Heat Transfer*, Vol. 109, 25-30.

[4] Berner C., Durst F.& McEligot D.M., 1984. Flow around baffles, *J. Heat Transfer*, Vol. 106, 743-749.

[5] Kim S.H.&Anand N.K., 1994. Turbulent heat transfer between a series of parallel plates with surface mounted discrete heat sources, *J. Heat Transfer*, Vol. 116, 577-587.

[6] Mohammadi Pirouz M., Farhadi M., Sedighi K., NematiH.&FattahiE. 2011. Lattice Boltzmann simulation of conjugate heat transfer in arectangular channel with wall-mounted obstacles, *Scientia Iranica B*,Vol. 18(2), 213-221.

[7] Dutta P.& Dutta S., 1998. Effect of baffle size, perforation, and orientation on internal heat transfer enhancement, *Int. J. Heat Mass Transfer*, Vol. 41, 3005-3013.

[8] Lopez J.R., Anand N.K.& Fletcher L.S., 1996. Heat transfer in a three-dimensional channel with baffles, *Numerical Heat Transfer A Appl.*, Vol. 30, 189-205.

[9] Guo Z.& Anand N.K., 1997. Three-dimensional heat transfer in a channel with a baffle in the entrance region, *Numerical Heat Transfer A Appl.*, Vol. 31(1), 21-35.

[10] Yang Y.T.& Hwang C.Z., 2003. Calculation of turbulent flow and heat transfer in a porous baffled channel, *Int. J. Heat Mass Transfer*, Vol. 46, 771-780.

[11] Da Silva Miranda B.M. & Anand N.K., 2004. Convective heat transfer in a channel with porous baffles, *Numerical Heat Transfer A Appl.*,Vol. 46(5), 425-452.

[12] Santos N.B. & De Lemos M.J.S., 2006. Flow and heat transfer in a parallel-plate channel with porous and solid baffles, *Numerical Heat Transfer A Appl.*, Vol. 49(5), 471-494.

[13] Ko K.H. & Anand N.K., 2003. Use of porous baffles to enhance heat transfer in a rectangular channel, *Int. J. Heat Mass Transfer*, Vol. 46,4191-4199.

[14] Tsay Y.L., Cheng J.C.& Chang T.S., 2003. Enhancement of heat transfer from surface mounted block heat sources in a duct with baffles, *Numerical Heat Transfer A Appl.*, Vol. 43(8), 827-841.

[15] Sripattanapipat S. & Promvonge P., 2009. Numerical analysis of laminar heat transfer in a channel with diamond-shaped baffles, *Int. Commun. Heat Mass Transfer*, Vol. 36 (1),32-38.

[16] Promvonge P., Sripattanapipat S., Tamna S., Kwankaomeng S. & Thianpong C., 2010. Numerical investigation of laminar heat transfer in a square channel with 45° inclined baffles, *Int. Commun. Heat Mass Transfer*, Vol. 37 (2), 170-177.

[17] Tang X.Y. & Zhu D.S., 2012. Experimental and numerical study on heat transfer enhancement of a rectangular channel with discontinuous crossed ribs and grooves, *Chin. J. Chem. Eng.*, Vol. 20(2), 220-230.

[18] Eiamsa-ard S., Koolnapadol N.& Promvonge P., 2012. Heat transfer behavior in a square duct with tandem wire coil element insert, *Chin. J. Chem. Eng.*, Vol. 20 (5), 863-869.

[19] Eiamsa-ard S., Kongkaitpaiboon V. & Nanan K., 2013. Thermo-hydraulics of turbulent flow through heat exchanger tubes fitted with circular-rings and twisted tapes, *Chin. J. Chem. Eng.*, Vol. 21(6), 585-593.

[20] Demartini L.C., Vielmo H.A. & Möller S.V., 2004. Numeric and experimental analysis of the turbulent flow through a channel with baffle plates, *J. of the Braz. Soc. of Mech. Sci. & Eng.*, Vol. 26,153-159.

[21]Nasiruddin & Kamran Siddiqui M.H., 2007. Heat transfer augmentation in a heat exchanger tube using a baffle, *Int. J. Heat Fluid Flow*, Vol.28, 318-28.

[22] Fluent Inc., 2006. User´s guide 6.3.

[23] Roache P.J., 1998. Verification and Validation in Computational Science and Engineering, Hermosa Publishers, Albuquerque, NM.

[24] Menter F.R., 1994. Two-equation eddy-viscosity turbulence models for engineering applications, *J. AIAA.*, Vol. 32, 8.

[25] Patankar S.V., 1980. Numerical heat transfer and fluid flow, McGraw-Hill, New York.

AUTHOR'S CONTRIBUTIONS

Each author of this manuscript made considerable contributions in developing the mathematical modeling, data-analysis and contributed to the writing of this manuscript.

NOMENCLATURE

Cf	Skin friction coefficient
D_h	Hydraulic diameter of rectangular channel, m
e	Waved-shaped baffle thickness, m
f	Friction factor
G_k	Turbulent kinetic energy generation due to mean velocity gradient
G_ω	Kinetic energy generation due to buoyancy
H	Channel height, m
h	Waved-shaped baffle height, m
h_x	Local convective heat transfer coefficient, W m^{-2} K^{-1}
K	Turbulent kinetic energy, m^2/s^2
L	Length of rectangular channel in x-direction, m
L_{in}	Distance upstream of the first waved-shaped baffle, m
L_{out}	Distance downstream of the second waved-shaped baffle, m
$\overline{Nu}$	Average Nusselt number
Nu_x	Local Nusselt number
P	Pressure, Pa
P_{atm}	Atmosphericpressure, Pa
Pr	Prandtl number
Re	Reynolds number based on the channel hydraulic diameter
S	Waved-shaped baffle distance or spacing, m
S_k, S_ω	Source term of k and ω
T	Temperature, °C
T_{in}	Inlet fluid temperature, °C
T_w	Wall temperature, °C
$\overline{U}$	Mean axial velocity of the section, m/s
U_{in}	Inlet velocity, m/s
u, v	Velocity component in x- and y-direction, m/s
u_i	Velocity component in x_i-direction, m/s
u_j	Velocity component in x_j-direction, m/s
x, y	Cartesian coordinates, m
Y_k, Y_ω	Dissipation of k and ω

Greek symbols

ω	Specific dissipation rate, m^2/s
Γ_k, Γ_ω	Effective diffusivity of k and ω
ρ	Fluid density, kg/m^3
μ	Dynamic viscosity, Kg/m s
μ_f	Fluid dynamic viscosity, Kg/m s
μ_t	Turbulent viscosity, Kg/m s

τ_w	Wall shear stress, Kg/s^2 m
λ_f	Fluid thermal conductivity, W/m°C
ΔP	Pressure drop, Pa

Subscript

atm	Atmospheric
f	Fluid
i, j	Refers coordinate direction vectors
in,	Inlet, outlet of the computational
out	domain
t	Turbulent
w	Wall
x	Local